Journal of
Materials Chemistry

Cite this: *J. Mater. Chem.*, 2012, **22**, 168

www.rsc.org/materials

PAPER

Laterally connected bent-core dimers and bent-core-rod couples with nematic liquid crystalline phases†

Govindaswamy Shanker, Marko Prehm and Carsten Tschierske*

Received 31st July 2011, Accepted 6th September 2011
DOI: 10.1039/c1jm13649f

First examples of laterally connected bent-core dimesogens and liquid crystalline dimesogens involving bent-core units and rod-like units are reported. Four distinct types of dimesogens have been synthesized and investigated by polarizing microscopy (PM), differential scanning calorimetry (DSC) and X-ray diffraction (XRD) studies. Two of them combine two bent-core mesogens derived from 4-cyanoresorcinol either in a lateral–lateral or lateral–terminal topology, the other two types combine a 4-cyanoresorcinol based bent-core mesogen with a rod-like mesogen in a lateral–lateral or lateral–terminal manner. All compounds, except one, exhibit nematic phases composed of SmC-type cybotactic clusters (N_{cybC}) with wide phase ranges and low crystallization temperatures. Two compounds show additional low temperature phases, an SmC phase and a rectangular columnar phase were observed.

1. Introduction

Liquid crystalline (LC) materials[1] are of great importance for different types of functional materials. Besides the well-known display applications also several new areas are rapidly emerging, as for example in charge carrier materials[2] and in biosensor applications[3] to mention only two. Among the distinct types of LC materials ranging from rod-like *via* disc-like to globular,[4] bent-core mesogens have attracted special attention due to their unique properties,[5] as for example, spontaneous polar order[5] and achiral symmetry breaking with formation of chiral superstructures despite the molecules being achiral.[6] In recent years the possibility of phase biaxiality in the nematic phases (N_b phases) of bent core molecules, caused by the restricted rotation of these molecules around the long axis, was discussed intensively.[7–10] N_b phases have attracted a lot of attention since their theoretical prediction[11] and their first observation in lyotropic LC systems.[12] These LC phases would be of fundamental interest for general soft matter physics as well as for use in display applications with a magnitude faster expected switching times than the existing uniaxial nematics.[13] Though there have been stimulating simulation results[14] and several different synthetic approaches to discover the illusive biaxial nematic phases by designing different kinds of molecules,[8] solid proof was only provided for polymeric LC[15] and laterally connected oligomesogen[16] in temperature ranges close to the glass transition temperature. However, the high viscosity of these polymers and oligomers under these conditions is disadvantageous for investigations and application.

Mesogenic dimers incorporating bent-core units could possibly provide a compromise as these compounds combine features of polymers/oligomesogens with those of low molecular mass mesogens, *i.e.* they interconnect and preorganize individual mesogenic units covalently, but still have relatively low molecular masses and viscosities. Previously reported dimers incorporating bent-core units represented exclusively end-to-end connected dimesogens (Scheme 1, left),[17] either composed of two bent-core mesogenic segments[18] or combining a rod-like unit with a bent-core unit.[19] Here we report the first examples of side-by-side and side-to-end connected bent-core dimesogens as well as related dimesogens composed of a bent-core unit combined with a laterally attached rod-like mesogenic core (Scheme 1, right). As bent-core mesogenic unit a 4-cyanoresorcinol bisbenzoate core was chosen, because this unit is known to favour formation of nematic phases.[10,20,21] The flexible spacer units consist of alkyl chains which, for synthetic reasons, contain a bis(dimethylsiloxane) unit in the middle.

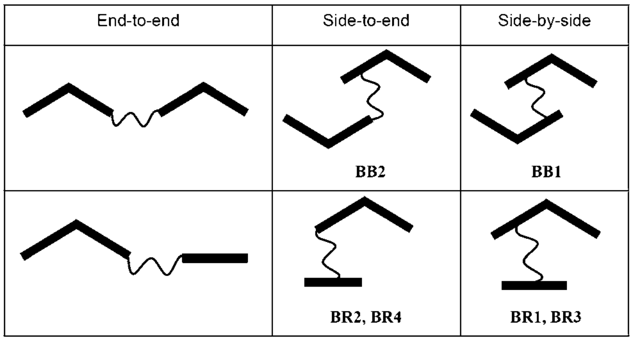

Scheme 1 Different types of bent-core dimesogens.

Institute of Chemistry, Organic Chemistry, Martin-Luther-University Halle-Wittenberg, Kurt Mothes Str. 2, D-06120 Halle/Saale, Germany. E-mail: carsten.tschierske@chemie.uni-halle.de; Fax: +49 0 345 55 27346

† Electronic supplementary information (ESI) available: See DOI: 10.1039/c1jm13649f

2. Experimental

2.1. Synthesis

As shown in Scheme 2, the bent-core dimesogens **BB1** and **BB2** and the bent-core-rod couples **BR1–BR4** were synthesized by hydrosilylation of the bent core compounds **B1–B3** with 1,1,3,3-tetramethyldisiloxane using Karstedt's catalyst.[17,22] The intermediate H-silanes **Si1–Si3** were isolated and immediately used[23] for the second hydrosilylation step with the olefin-functionalized bent-core mesogens **B1** and **B3** to give the bent-core dimesogens **BB1** and **BB2**, or they were used in hydrosilylation reactions with the laterally olefin-functionalized rod-like molecules **R1** and **R2** to give the bent-core-rod couples **BR1–BR4**. All dimesogens were purified by column chromatography and the structures were confirmed by ^{1}H NMR and ^{13}C NMR (see Fig. S1 and S2†). Details of the synthetic procedures and analytical data are collated in the ESI†. The olefin substituted bent-core mesogen **B3** will be reported separately[24] and the naphthalene based rod-like unit **R2**[25] was kindly provided by F. Brömmel and A. Hoffmann, University Freiburg.

2.2. Investigations

The obtained dimers were investigated by PM (Optiphot 2, Nikon) in conjunction with a heating stage (FP82HT, Mettler) and by DSC (DSC-7 Perkin Elmer). The assignment of the mesophases was made on the basis of combined results of optical textures and X-ray diffraction (XRD). Investigations of oriented samples were performed using a 2D detector (H1-Star, Siemens AG). Uniform orientation was achieved by alignment in a magnetic field ($B \approx$ 1T) using thin capillaries. The orientation once achieved is maintained by slow cooling (0.1 K min^{-1}) in the presence of the magnetic field. Electro-optical experiments have been carried out using a home built electro-optical setup in commercially available ITO coated glass cells (E.H.C., Japan, polyimide coated for planar alignment, antiparallel rubbing, thickness 6 μm and measuring area 1 cm^2).

3. Results and discussion

3.1. Mesophases and transition temperatures

The detailed structures, phase transition temperatures, transition enthalpies and phase sequences of the synthesized dimesogens are summarized in Fig. 1–3 and Table 1. All compounds exhibit liquid crystalline behaviour except the dimesogen **BR3** which has a naphthalene based rod-like unit connected to the bent-core moiety in a lateral–lateral mode (Table 1). A short monotropic nematic phase range was observed for the lateral–lateral connected bent-core dimer **BB1** (Table 1). All other dimesogens show broad regions of nematic phases. On cooling from the isotropic liquid state these LC phases appear with a schlieren

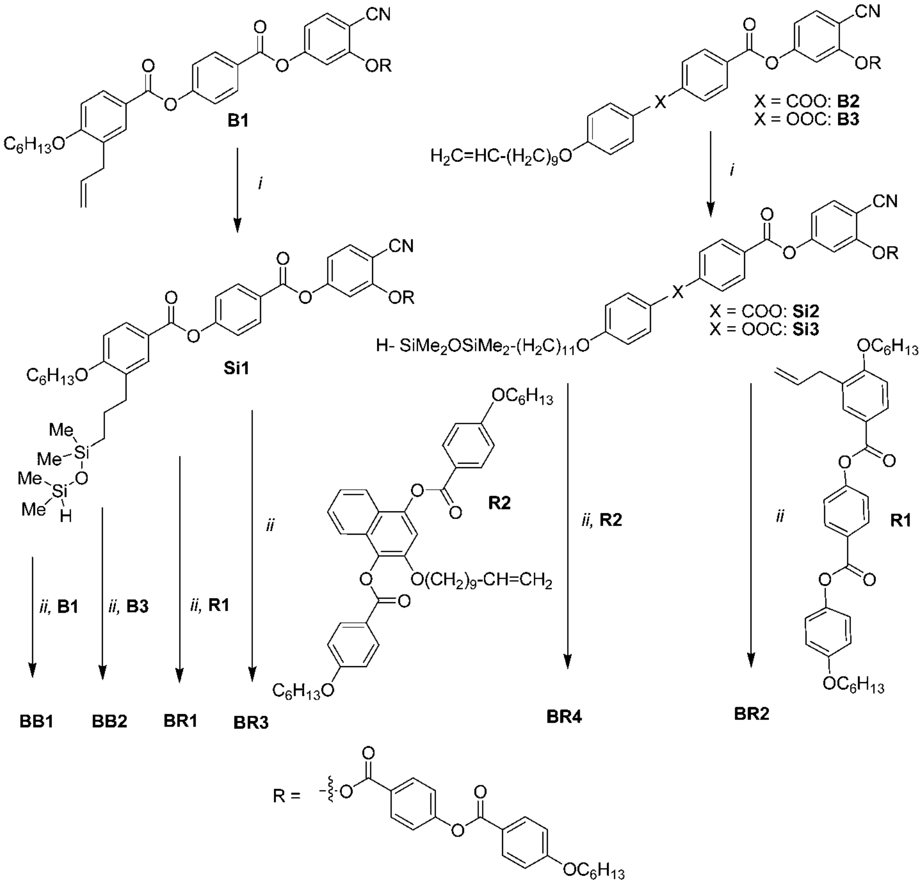

Scheme 2 Synthesis of compounds **BB1**, **BB2** and **BR1–BR4**; *reagents and conditions*: (i) H–Me$_2$SiOMe$_2$Si–H, Karstedt's catalyst, dry toluene, T = 25 °C, 12 h, (ii) Karstedt's catalyst, dry toluene, T = 25 °C, 12 h.[22]

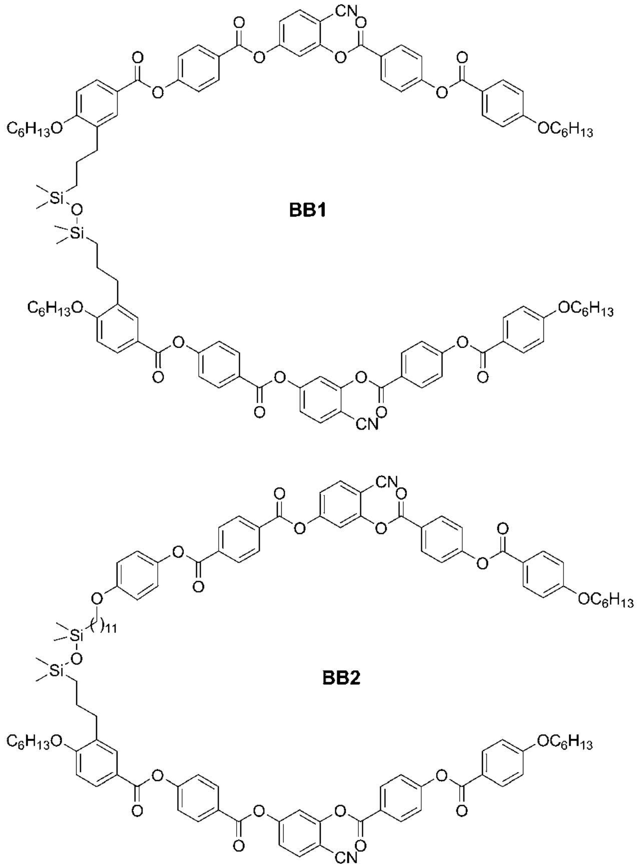

Fig. 1 Structures of the bent-core dimesogens **BB1** and **BB2**.

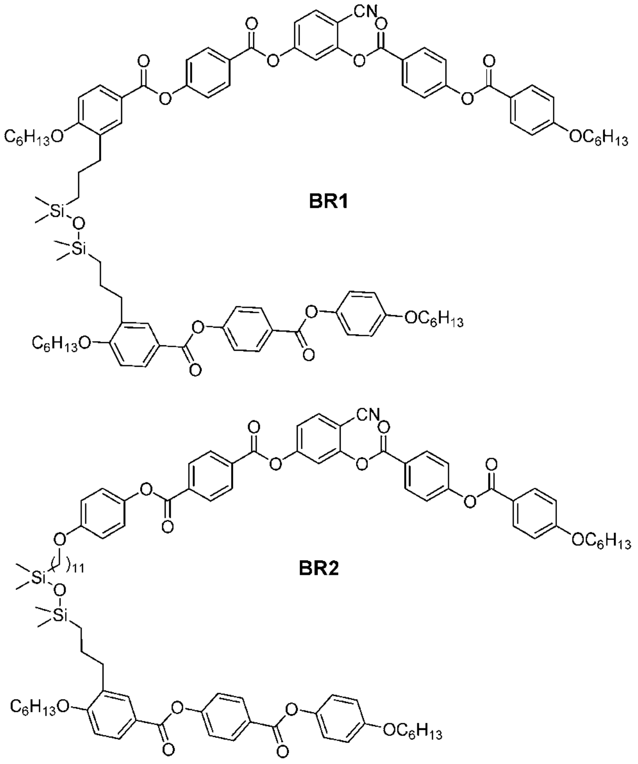

Fig. 2 Structures of dimesogens **BR1** and **BR2** combining a rod-like and a bent-core unit.

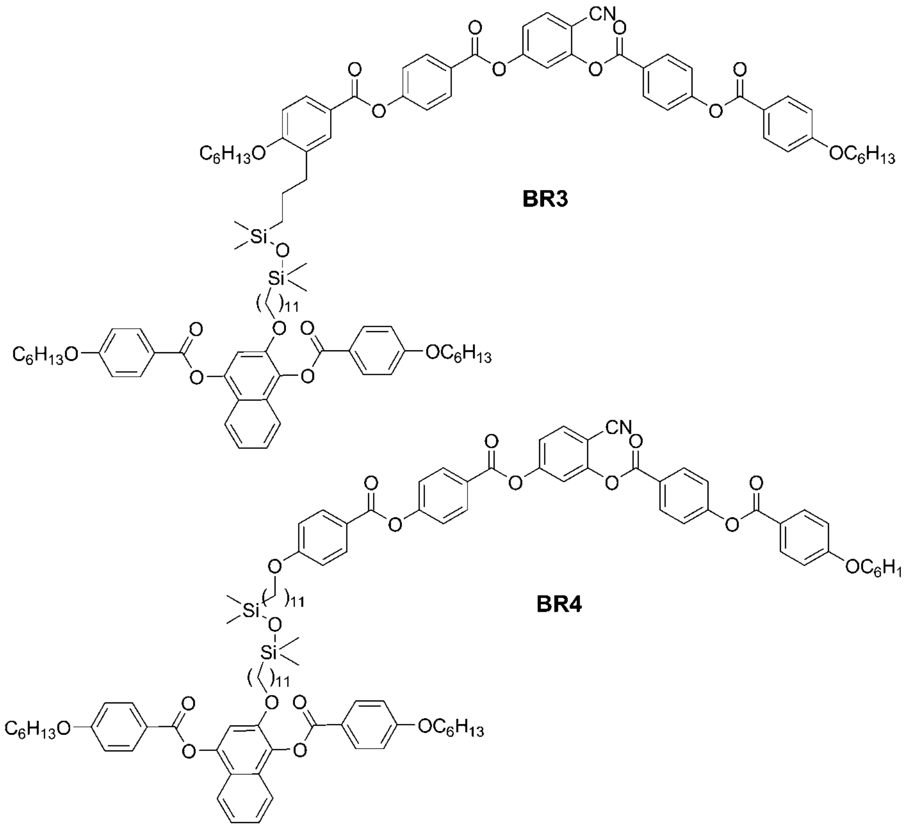

Fig. 3 Structures of dimesogens **BR3** and **BR4** combining a naphthalene based rod-like unit with a bent-core unit.

Table 1 Phase transition temperatures (T/°C), associated enthalpy values [ΔH/kJ mol^{-1}] and crystallization temperatures (T_{Cr}/°C) of the bent-core dimesogens **BB1**, **BB2** and bent-core-rod couples **BR1–BR4**[a]

Comp.	Phase transitions	T_{cr}
BB1	Cr 84 [54.9] (N 68 [0.2]) Iso	41
BB2	Cr 94 [63.2] (SmC 44 [5.2]) N_{cybC} 117 [1.1] Iso	35
BR1	Cr 53 [22.8] N_{cybC} 71 [0.6] Iso	<20
BR2	Cr 51 [11.0] (Col_{rec} 47 [5.4]) N_{cybC} 100 [0.5] Iso	<20
BR3	Cr 40 [18.3] Iso	<20
BR4	Cr 32 [15.4] (M 22 [3.2]) N_{cybC} 84 [1.4] Iso	<20

[a] Peak temperatures in the DSC thermograms obtained during first heating and cooling cycles at 10 K min^{-1}, monotropic phase transitions and crystallization temperatures were taken from the corresponding cooling scans (10 K min^{-1}); Abbreviations: Cr = crystalline solid; N = nematic phase; SmC = smectic C phase; N_{cybC} = nematic phase composed of SmC type cybotactic clusters; M = mesophase with unknown structure; Col_{rec} = rectangular columnar phase; Iso = isotropic liquid; for **BR1–BR4** compounds no crystallization peak was observed by DSC down to −20 °C.

texture containing π/2 and π/4 disclinations and marble domains as typical for nematic phases. A typical texture is shown in Fig. 4a for the nematic phase of compound **BR2** as example.

For compound **BR1** (Table 1), combining a rod-like phenylbenzoate unit with the bent-core unit in a side-by-side fashion *via* a relatively short spacer unit, the nematic phase can be overcooled down to −20 °C. No transition to a smectic or columnar phase was observed, despite the incorporation of a bis(dimethylsilyl)oxy unit which is expected to have a certain tendency for micro-segregation.[4,17] All other mesogenic compounds with longer spacer units can also be cooled down below room temperature without crystallization, but in these cases additional phase transitions were observed. For **BR2**, the low temperature phase is a rectangular columnar phase as evidenced by XRD (see below) and also by DSC thermograms (Fig. S3a†). The lateral–terminal connected bent-core dimer **BB2** (Table 1) exhibits a short range SmC phase (Fig. S3b†) on cooling before crystallization.

The highest stability of the nematic phase was observed for compounds **BB2**, **BR2** and **BR4** in which the bent-core unit is coupled at the end with a laterally attached rod-like unit or a laterally attached second bent-core unit. In contrast, lateral attachment of the bent-core unit is generally unfavourable for mesophase formation giving crystalline material (**BR3**) or lower transition temperatures (**BB1** and **BR1**) and shorter temperature ranges of the N phases.

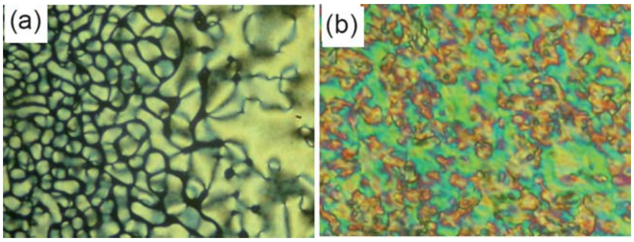

Fig. 4 Textures of **BR2** as observed between crossed polarizers (a) N_{cybC} at T = 99 °C and (b) in the Col_{rec} phase at T = 40 °C.

3.2. XRD studies

XRD studies were carried out with magnetically aligned samples of the dimesogens **BB2**, **BR1**, **BR2** and **BR4**. In the temperature range of the nematic phases all XRD patterns show a diffuse scattering in the wide angle region with a maximum at d = 0.46–0.47 nm, indicating fluid LC phases. The maximum is located on the equator (Fig. 5a and 6a and c) indicating an alignment of the molecules with the long axes of the aromatic cores parallel to the magnetic field direction. The diffuse scattering in the small angle region indicates that there is only short range periodicity as typical for nematic phases. The intensity of the small angle scattering is in the same range or larger than the intensity of the wide angle scattering ($I_w \leq I_s$), indicating the presence of cybotactic groups.[26] This scattering is smeared out to dumbbell-shaped streaks parallel to the equator with four distinct maxima located beside the meridian (see Fig. 5c and 6d). This shape of the small angle scattering indicates cybotactic nematic phases formed by tilted (SmC-like) clusters (N_{cybC} phases).[10]

For compound **BB2** (Fig. 5) the correlation length, estimated according to $\xi_{\parallel,\perp} = 2/\Delta q$ from the full width at half maximum (Δq)[27] of the small angle scatterings in the transversal direction is $\xi_{\parallel}$ = 2.7 nm and in longitudinal direction it is $\xi_{\perp}$ = 3.2 nm. The dimensions of the cybotactic clusters ($L_{\parallel,\perp}$) can be approximated to $L_{\parallel,\perp} \approx 3\xi_{\parallel,\perp}$,[28] leading to the values $L_{\parallel} \approx$ 8 nm and $L_{\perp} \approx$ 3 to 4 nm for the cluster size. Accordingly, the cybotactic clusters in the N_{cybC} phase of **BB2** are composed on average of about 2 layers and about 7–8 aromatic cores are arranged in the cross-section.[26] Similar values were obtained for compounds **BR2** and **BR4** (Fig. S5†) (see Table 2). Only for **BR1** (Fig. S4†) the cluster size is smaller than for those of the other compounds (thickness of only one layer). The temperature dependence of the cluster size was investigated for compound **BR4** and, as expected, the size decreases with rising temperature.[10] The splitting of the small

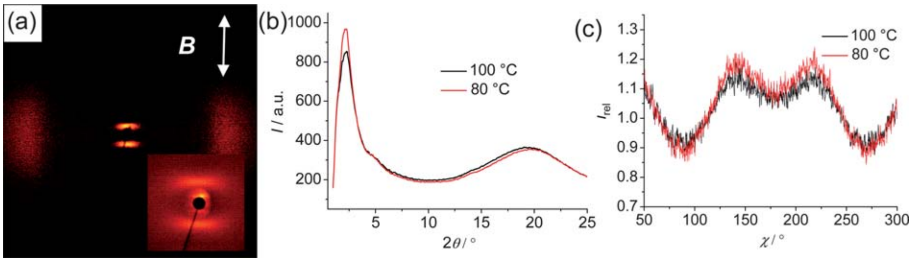

Fig. 5 (a) Diffraction pattern of a magnetically aligned sample (direction of the magnetic filed is shown as white arrow) of **BB2** at 80 °C after subtraction of the scattering pattern in the Iso phase at T = 120 °C (the inset shows the scattering in the small angle region); (b) θ-scans at 100 °C and 80 °C; (c) χ-scans over the diffuse small angle scattering (for 2θ = 1.5–4.5°), $I_{rel} = I(T)/I(120\ °C, \text{Iso})$.

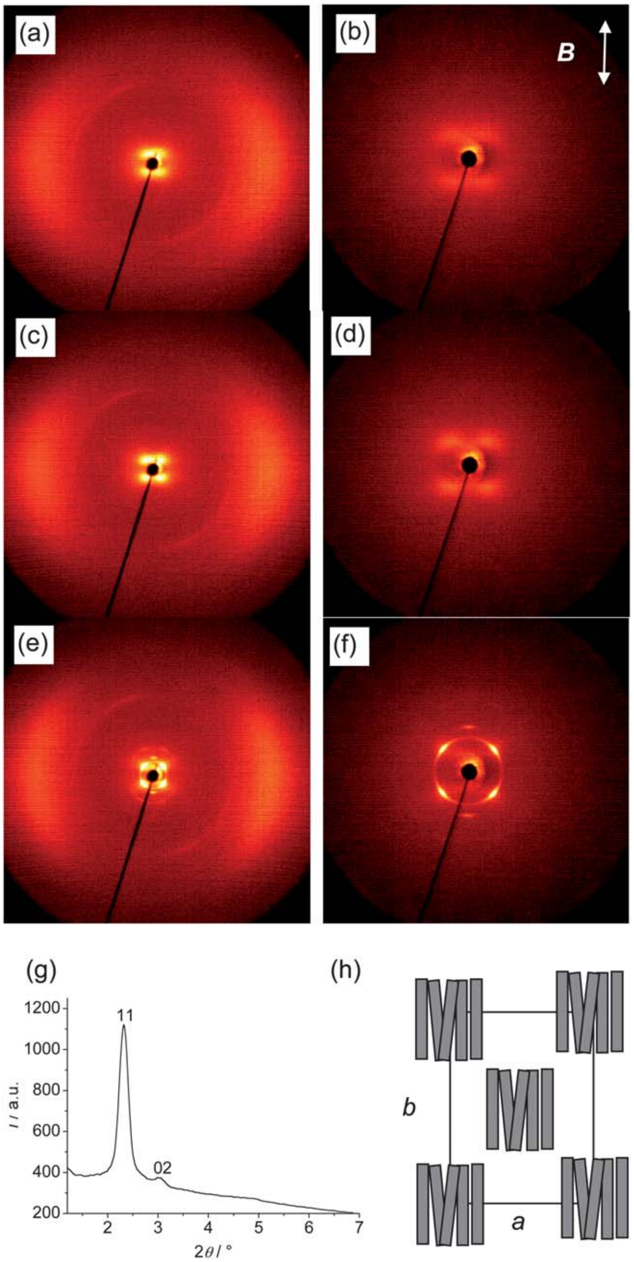

Fig. 6 XRD investigation of an aligned sample of compound **BR2** (a and b) N_{cybC} phases at $T = 90$ °C; (c and d) at $T = 60$ °C and (e and f) Col_{rec} phase $T = 40$ °C; (a, c and e) show the complete diffraction patterns, (b, d and f) the small angle region; (g) θ-scan of diffraction pattern shown in (f), and (h) model showing the proposed organization of bent-core units (rotationally disordered around their long axes) on a rectangular lattice.

angle scattering $\Delta\chi/2$ is between 35° (**BR4**) and 50° (**BR1**) indicating that there is a significant tilt of the molecules in the SmC-like clusters.[10] The position of the maximum of the small angle scattering is between $d = 3.2$ nm for the bent-core dimesogen **BR1** and $d = 4.6$ for the mixed dimesogen **BR2**. The value of $d = 3.2$ nm is in good agreement with the distances typically observed for the small angle reflection in the nematic phases of comparable single mesogens (*e.g.* compound **B7** in Table 2). The difference between the d-values of the dimesogen **BR1** ($d = 3.2$ nm) and the monomeric compound **B7** ($d = 3.8$ nm)[10] results from the much larger tilt of the dimesogen, which is nearly double compared to **B7**. For the other dimesogens it is more difficult to evaluate the ratios between d-value and molecular length, as the length of the two aromatic units is different and for dimesogens with a connection *via* the end of the bent core unit it is also difficult to estimate the effective molecular size as one of the terminal chains simultaneously acts as a spacer unit and this should have a significant effect on chain conformation.

As shown in Fig. 6a–d for the XRD patterns of compound **BR2** the intensity of the small angle scattering increases as the temperature is reduced, indicating increasing cluster size at lower temperature (see also Table 2). At $T = 47$ °C a phase transition takes place (see Fig. 4b for the textural change) and below this temperature the XRD pattern is significantly changed (Fig. 6e–g). The wide angle scattering remains diffuse, indicating that the low temperature phase is also a fluid LC phase. However, the diffuse small angle scattering becomes a sharp Bragg peak and an additional reflection occurs on the meridian. This diffraction pattern can be indexed on a centred rectangular lattice (*c*2*mm*) with the parameters $a = 5.05$ and $b = 5.81$ nm ($T = 40$ °C). The diffuse wide angle scattering does not split at this phase transition and remains centered on the equator. Therefore, the aromatic cores should be organized with their long axes parallel to the direction b (Fig. 6h). This is also in agreement with the increase of the d-value for the small angle scattering from $d = 4.5$ nm in the nematic phase to $d = 5.81$ nm in the low temperature phase. This alignment of the cores and the presence of a rectangular 2D lattice indicate that the molecules are organized perpendicular to the (broken) layers of a modulated smectic phase. The parameter $a/2$ corresponds to the lateral distance between ribbon-like blocks of molecules and indicates that the diameter of each ribbon is about 2.5 nm, which correspond to roughly five aromatic units arranged side by side. This is less than half the value of the estimated lateral dimension $L_\perp = 6.6$ nm of the cybotactic clusters in the nematic phase at $T = 60$ °C. Hence, at this transition the cybotactic clusters of the N_{cybC} phase change their shape and form quasi-infinite ribbons which organize on a *c*2*mm* type 2D lattice (see Fig. 6h).

It is a bit surprising that the relatively strong tilt in the SmC-clusters is completely removed at this phase transition.[29] It is not clear if in the ribbons the molecules adopt polar order along direction c, with antiparallel alignment of the polar direction between adjacent ribbons, as typically observed for $B1_{rev}$

Table 2 XRD data of the nematic phases of compounds **BB2**, **BR1**, **BR2** and **BR4** and the reference compound **B7**[10] having the same structure of the bent-core mesogen as used in compound **BB1**, but with two C_7H_{15} chains instead of the OC_6H_{13} chains

Comp.	T/°C	d/nm	$\Delta\chi/2$/°	d/nm	$L_\perp$/nm	$L_\parallel$/nm
BR4	80	4.1	35	0.47	5.1	6.6
BR4	60	4.5	38	0.46	6.5	9.0
BR4	40	4.4	39	0.46	7.2	10.3
BR2	90	4.6	42	0.47	5.8	9.3
BR2	60	4.5	44	0.47	6.6	8.8
BR1	65	3.2	50	0.47	3.0	3.5
BB2	80	4.2	39	0.46	3.5	8.2
B7[10]	70	3.8	26	0.45	3.7	14.0

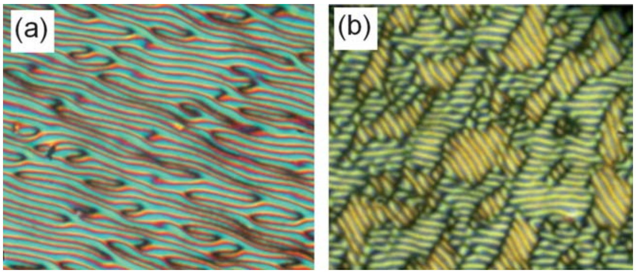

Fig. 7 Electrohydrodynamic instabilities as seen for the nematic phase of **BR2** in a 6 μm polyimide coated ITO cell (a) at T = 75 °C, 10 Hz, 160 Vpp and (b) at T = 75 °C, 10 Hz, 200 Vpp.

phases,[30] or if the bent aromatic cores are rotationally disordered around their long axes. As in electro-optical investigations no polarization current peak could be recorded (see below) and in compound **BR2** the bent-core mesogens are diluted in the ratio 1 : 1 with rod-like mesogens it appears more likely that polar order is absent (see Fig. 6h).

3.3. Electro-optical investigations

As reported for other bent-core mesogens[19c,d,31] in the nematic phase, often a frequency dependent reversal of the dielectric anisotropy can be found. However, in the nematic phase ranges of the compounds reported here only highly birefringent planar alignment was obtained at 1 kHz accompanied with formation of electro-convection patterns as evidence of strong hydrodynamic instabilities (Fig. 7), indicating that the dielectric anisotropy is negative. Even on varying frequency (0.02 Hz–5 kHz.) and voltage (2–200 Vpp), as checked for compound **BR2**, we were unable to obtain homeotropic alignment and therefore it was not possible to check phase biaxiality in the nematic phases.[31] Also by investigation with polarized IR no macroscopic biaxiality was observed in the nematic phases of **BR1** and **BB2** as representative examples.[32] It should also be noted that in the entire nematic phase range there was no polar switching under an applied triangular wave field even at high voltage (200 Vpp, 6 μm ITO cell, Fig. S6†). Hence, in the LC phases of these compounds the aromatic cores do not adopt polar order.

4. Conclusion

First examples of laterally connected bent-core dimesogens and dimesogens combining a bent-core unit with a rod-like unit have been synthesized and investigated. These dimesogens have broad nematic phase ranges (enantiotropic and monotropic) and low crystallization tendency if they are lateral–terminal connected, whereas a lateral–lateral connection reduces the nematic phase stability. Compounds with short end-chains and short spacer units can provide nematic phases at ambient temperature, which do not show transitions to other LC phases down to −20 °C, whereas compound **BR2** forms a rectangular columnar low temperature phase. Though distinct modes of connection either lateral–lateral or lateral–terminal have been checked, according to preliminary investigations no evidence of biaxiality in the nematic phases of these molecules could be provided, even for the two dimesogens incorporating a board-like unit (**BR3** and **BR4**). This would mean that the laterally connected bent-core dimesogens reported herein do not provide that degree of coupling which would be required for phase biaxiality to occur. Probably, by reduction of the spacer length and spacer flexibility a stronger coupling could be achieved, which is presently under investigation.

Acknowledgements

This work was supported by the EU within the FP7 funded Collaborative Project BIND (Grant No 216025); we are grateful to F. Brömmel and A. Hoffmann, University Freiburg for providing us compound **R2**.

References

1 *Handbook of Liquid Crystals*, ed. D. Demus, J. Goodby, G. W. Gray, H.-W. Spiess and V. Vill, Wiley-VCH, Weinheim, 1998.
2 M. O. Neill and S. M. Kelly, *Adv. Mater.*, 2011, **23**, 566–584.
3 (*a*) S. Sivakumar, K. L. Wark, J. K. Gupta, N. L. Abbott and F. Caruso, *Adv. Funct. Mater.*, 2009, **19**, 2260–2265; (*b*) A. Agarwal, E. Huang, S. Palecek and N. L. Abbott, *Adv. Mater.*, 2008, **20**, 4804–4809; (*c*) A. Angelova, B. Angelov, R. Mutafchieva, S. Lesieur and P. Couvreur, *Acc. Chem. Res.*, 2011, **44**, 147–156.
4 (*a*) C. Tschierske, *J. Mater. Chem.*, 1998, **8**, 1485–1508; (*b*) C. Tschierske, *J. Mater. Chem.*, 2001, **11**, 2647–2671; (*c*) J. W. Goodby, I. M. Saez, S. J. Cowling, V. Görtz, M. Draper, A. W. Hall, S. Sia, G. Cosquer, S. E. Lee and E. P. Raynes, *Angew. Chem., Int. Ed.*, 2008, **47**, 2754–2787.
5 (*a*) T. Niori, T. Sekine, J. Watanabe, T. Furukawa and H. Takezoe, *J. Mater. Chem.*, 1996, **6**, 1231–1233; (*b*) D. R. Link, G. Natale, R. Shao, J. E. Maclennan, N. A. Clark, E. Körblova and D. M. Walba, *Science*, 1997, **278**, 1924–1927; (*c*) R. Amaranatha Reddy and C. Tschierske, *J. Mater. Chem.*, 2006, **16**, 907–961; (*d*) H. Takezoe and Y. Takanishi, *Jpn. J. Appl. Phys.*, 2006, **45**, 597–625; (*e*) J. Etxebarria and M. B. Ros, *J. Mater. Chem.*, 2008, **18**, 2919–2929; (*f*) G. Pelzl and W. Weissflog, in *Thermotropic Liquid Crystals: Recent Advances*, ed. A. Ramamoorthy, Springer, Berlin, 2007, pp. 1–58.
6 (*a*) T. Sekine, T. Niori, J. Watanabe, T. Furukawa, S. W. Choi and H. Takezoe, *J. Mater. Chem.*, 1997, **8**, 1307–1309; (*b*) L. E. Hough, M. Spannuth, M. Nakata, D. A. Coleman, C. D. Jones, G. Dantlgraber, C. Tschierske, J. Watanabe, E. Körblova, D. M. Walba, J. E. Maclennan, M. A. Glaser and N. A. Clark, *Science*, 2009, **325**, 452–456; (*c*) C. Tschierske, in *Chirality at the Nano Scale*, ed. D. B. Amabiliino, Wiley-VCH, Weinheim, 2009, p. 271.
7 (*a*) C. Tschierske and D. J. Photinos, *J. Mater. Chem.*, 2010, **20**, 4263–4294; (*b*) A. G. Vanakaras and D. J. Photinos, *J. Chem. Phys.*, 2008, **128**, 154512-6; (*c*) S. D. Peroukidis, P. K. Karahaliou, A. G. Vanakaras and D. J. Photinos, *Liq. Cryst.*, 2009, **36**, 727–737; (*d*) P. K. Karahaliou, A. G. Vanakaras and D. J. Photinos, *J. Chem. Phys.*, 2009, **131**, 124516-14.
8 (*a*) G. R. Luckhurst, *Thin Solid Films*, 2001, **393**, 40–52; (*b*) K. Praefcke, *Mol. Cryst. Liq. Cryst. Sci. Technol., Sect. A*, 2001, **364**, 15–24; (*c*) G. R. Luckhurst, *Angew. Chem., Int. Ed.*, 2005, **44**, 2834–2836; (*d*) D. W. Bruce, *Chem. Rec.*, 2004, **4**, 10–22.
9 (*a*) L. A. Madsen, T. J. Dingemans, M. Nakata and E. T. Samulski, *Phys. Rev. Lett.*, 2004, **92**, 145505-1; (*b*) L. A. Madsen, T. J. Dingemans, M. Nakata and E. T. Samulski, *Phys. Rev. Lett.*, 2006, **96**, 219804-1; (*c*) O. Francescangeli and E. T. Samulski, *Soft Matter*, 2010, **6**, 2413–2420; (*d*) M. Lehmann, C. Köhn, H. Kresse and Z. Vakhovskaya, *Chem. Commun.*, 2008, 1768–1770; (*e*) P. J. Martin and D. W. Bruce, *Liq. Cryst.*, 2007, **34**, 767–774; (*f*) S.-W. Choi, S. Kang, Y. Takanishi, K. Ishikawa, J. Watanabe and H. Takezoe, *Chirality*, 2007, **19**, 250–254; (*g*) V. Görtz and J. W. Goodby, *Chem. Commun.*, 2005, 3262–3264; (*h*) Y. Xiang, J. W. Goodby, V. Görtz and H. F. Gleeson, *Appl. Phys. Lett.*, 2009, **94**, 193507-3.
10 C. Keith, A. Lehmann, U. Baumeister, M. Prehm and C. Tschierske, *Soft Matter*, 2010, **6**, 1704–1721.

11 M. J. Freiser, *Phys. Rev. Lett.*, 1970, **24**, 1041–1043.

12 L. J. Yu and A. Saupe, *Phys. Rev. Lett.*, 1980, **45**, 1000–1003.

13 R. Berardi, L. Muccioli and C. Zannoni, *J. Chem. Phys.*, 2008, **128**, 024905-12.

14 (*a*) R. Berardi, L. Muccioli, S. Orlandi, M. Ricci and C. Zannoni, *J. Phys.: Condens. Matter*, 2008, **20**, 463101-16; (*b*) T. C. Lubensky and L. Radzihovsky, *Phys. Rev. E: Stat., Nonlinear, Soft Matter Phys.*, 2002, **66**, 031704-5; (*c*) J. Pelaez and M. R. Wilson, *Phys. Rev. Lett.*, 2006, **97**, 267801-4.

15 (*a*) H. F. Leube and H. Finkelmann, *Makromol. Chem.*, 1991, **192**, 1317–1329; (*b*) K. Severing and K. Saalwächter, *Phys. Rev. Lett.*, 2004, **92**, 125501-4; (*c*) R. Storz, A. Komp, A. Hoffmann and H. Finkelmann, *Macromol. Rapid Commun.*, 2009, **30**, 615–621.

16 (*a*) K. Merkel, A. Kocot, J. K. Vij, R. Korlacki, G. H. Mehl and T. Meyer, *Phys. Rev. Lett.*, 2004, **93**, 237801-4; (*b*) G. Cordoyiannis, D. Apreutesei, G. H. Mehl, C. Glorieux and J. Thoen, *Phys. Rev. E: Stat., Nonlinear, Soft Matter Phys.*, 2008, **78**, 011708.

17 Bent-core 1,3,4-oxadiazoles with lateral siloxane units have been reported previously which could serve as precursors of laterally connected bent-core mesogens: D. Apreutesei and G. H. Mehl, *J. Mater. Chem.*, 2007, **17**, 4711–4715.

18 (*a*) G. Dantlgraber, S. Diele and C. Tschierske, *Chem. Commun.*, 2002, 2768–2769; (*b*) C. Keith, R. A. Reddy, U. Baumeister, H. Hahn, H. Lang and C. Tschierske, *J. Mater. Chem.*, 2006, **16**, 3444–3447; (*c*) R. Achten, A. Koudijs, M. Giesberg, A. T. M. Marcelis, E. J. R. Sudholter, M. W. Schröder and W. Weissflog, *Liq. Cryst.*, 2007, **34**, 59–64; (*d*) B. Kosata, M. G. Tamba, U. Baumeister, K. Pelz, S. Diele, G. Pelzl, G. Galli, S. Samaritani, E. V. Agina, N. I. Boiko, V. P. Shibaev and W. Weissflog, *Chem. Mater.*, 2006, **18**, 691–701; (*e*) S. Umadevi, B. K. Sadashiva, H. N. S. Murthy and V. A. Raghunathan, *Soft Matter*, 2006, **2**, 210–214; (*f*) S. Umadevi and B. K. Sadashiva, *Liq. Cryst.*, 2007, **34**, 673–681.

19 (*a*) S. K. Prasad, G. G. Nair, D. S. Shankar Rao, C. V. Lobo, I. S. Shashikala and C. V. Yelamaggad, *Mol. Cryst. Liq. Cryst.*, 2005, **437**, 211–221; (*b*) C. V. Yelamaggad, S. K. Prasad, G. G. Nair, I. S. Shashikala, D. S. S. Rao, C. V. Lobo and S. Chandrasekhar, *Angew. Chem., Int. Ed.*, 2004, **43**, 3429–3432; (*c*) C. V. Yelamaggad, S. A. Nagamani, U. S. Hiremath and G. G. Nair, *Liq. Cryst.*, 2001, **28**, 1009–1015; (*d*) A. Jakli, G. Liao, I. S. Shashikala, U. S. Hiremath and C. V. Yelamaggad, *Phys. Rev. E: Stat., Nonlinear, Soft Matter Phys.*, 2006, **74**, 041706-1; (*e*) M. G. Tamba, B. Kosata, K. Pelz, S. Diele, G. Pelzl, Z. Vakhovskaya, H. Kresse and W. Weissflog, *Soft Matter*, 2006, **2**, 60–65; (*f*) G. Leea, H.-C. Jeonga, F. Araoka, K. Ishikawa, J. G. Lee, K.-T. Kang, M. Cepic and H. Takezoe, *Liq. Cryst.*, 2010, **37**, 883–892; (*g*) P. Kumar, U. S. Hiremath, C. V. Yelamaggad, A. G. Rossberg and K. S. Krishnamurthy, *J. Phys. Chem. B*, 2008, **112**, 9753–9760; (*h*) P. Kumar, U. S. Hiremath, C. V. Yelamaggad, A. G. Rossberg and S. Krishnamurthy, *J. Phys. Chem. B*, 2008, **112**, 9270–9274; (*i*) M.-G. Tamba, W. Weissflog, A. Eremin, J. Heuer and R. Stannarius, *Eur. Phys. J. E*, 2007, **22**, 85–95; (*j*) C. V. Yelamaggad, I. S. Shashikala, G. Liao, D. S. S. Rao, S. K. Prasad, Q. Li and A. Jakli, *Chem. Mater.*, 2006, **18**, 6100–6102; (*k*) G. Liao, I. S. Shashikala, C. V. Yelamaggad, D. S. S. Rao, S. K. Prasad and A. J. Jákli, *Phys. Rev. E: Stat., Nonlinear, Soft Matter Phys.*, 2006, **73**, 051701-4; (*l*) J. Heuer, R. Stannarius, M.-G. Tamba and W. Weissflog, *Phys. Rev. E: Stat., Nonlinear, Soft Matter Phys.*, 2008, **77**, 056206-1; (*m*) R. Stannarius and J. Heuer, *Eur. Phys. J. E*, 2007, **24**, 27–33; (*n*) R. Stannarius, A. Eremin, M.-G. Tamba, G. Pelzl and W. Weissflog, *Phys. Rev. E: Stat., Nonlinear, Soft Matter Phys.*, 2007, **76**, 061704-1; (*o*) M.-G. Tamba, U. Baumeister, G. Pelzl and W. Weissflog, *Liq. Cryst.*, 2010, **37**, 853–874.

20 L. Kovalenko, M. W. Schröder, R. Amaranatha Reddy, S. Diele, G. Pelzl and W. Weissflog, *Liq. Cryst.*, 2005, **32**, 857–865.

21 (*a*) C. Keith, M. Prehm, Y. P. Panarin, J. K. Vij and C. Tschierske, *Chem. Commun.*, 2010, **46**, 3702–3704; (*b*) M. Nagaraj, Y. P. Panarin, J. K. Vij, C. Keith and C. Tschierske, *Appl. Phys. Lett.*, 2010, **97**, 213505-2; (*c*) Y. P. Panarin, M. Nagaraj, J. K. Vij, C. Keith and C. Tschierske, *Europhys. Lett.*, 2010, **92**, 26002.

22 (*a*) R. Elsasser, G. H. Mehl, J. W. Goodby and M. Veith, *Angew. Chem., Int. Ed.*, 2001, **40**, 2688–2690; (*b*) G. H. Mehl and J. W. Goodby, *Liq. Cryst.*, 1999, **26**, 1101–1105.

23 These intermediates are unstable but can be stored below °0 C for a day or two.

24 G. Shanker, M. Prehm, M. Nagaraj, J. K. Vij and C. Tschierske, *J. Mater. Chem.*, DOI: 10.1039/c1jm14653j.

25 A. Komp and H. Finkelmann, *Macromol. Rapid Commun.*, 2007, **28**, 55–62.

26 (*a*) A. de Vries, *Pramana*, 1975, **1**(Suppl), 93; (*b*) A. de Vries, *J. Mol. Liq.*, 1986, **31**, 193–202.

27 A. Guinier, *X-Ray Diffraction*, Freeman, San Francisco, 1963.

28 O. Francescangeli, M. Laus and G. Galli, *Phys. Rev. E: Stat. Phys., Plasmas, Fluids, Relat. Interdiscip. Top.*, 1997, **55**, 481–487.

29 (*a*) $\text{N-Col}_{\text{rec}}$ transitions have been observed previously, but in these cases the nematic phases were of the N_{CybA} type or the structure of the N phase was not investigated in detail: M. W. Schröder, S. Diele, G. Pelzl, U. Dunemann, H. Kresse and W. Weissflog, *J. Mater. Chem.*, 2003, **13**, 1877; (*b*) R. Amaranatha Reddy, B. K. Sadashiva and V. A. Raghunathan, *Chem. Mater.*, 2004, **16**, 4050–4062; (*c*) R. Amaranatha Reddy and B. K. Sadashiva, *J. Mater. Chem.*, 2004, **14**, 1936.

30 E. Gorecka, N. Vaupotic, D. Pociecha, M. Cepic and J. Mieczkowski, *ChemPhysChem*, 2005, **6**, 1087–1093.

31 K. V. Le, M. Mathews, M. Chambers, J. Harden, Q. Li, H. Takezoe and A. Jakli, *Phys. Rev. E: Stat., Nonlinear, Soft Matter Phys.*, 2009, **79**, 030701.

32 M. Nagaraj, V. P. Panov, J. Vij, G. Shanker and C. Tschierske, *Liq. Cryst.*, submitted.